Proteomic analysis revealed the function of PoElp3 in development, pathogenicity and autophagythrough the tRNA-mediated translation efficiency in the rice blast fungus

Ting Sun[1,†], Yuyong Li[1,†], Yuanhao Liu[1,†], Xianjun Wang[2], Jiahui Xie[2], Huimin Bai[2], Jiayi Hu[2], Zifan Zhang[1], Xiuxiu Li[2], Zonghua Wang[4,*], Huakun Zheng[1,*], Guifang Lin[3,*]

[1] Fujian Universities Key Laboratory for Plant Microbe Interaction, College of Life Sciences, Fujian Agriculture and Forestry University, Fuzhou 350002, China.

[2] State Key Laboratory of Ecological Pest Control for Fujian and Taiwan Crops, College of Plant Protection, Fujian Agriculture and Forestry University, Fuzhou 350002, China.

[3] Basic Forestry and Proteomics Research Center, Fujian Agriculture and Forestry University, Fuzhou, 350002, China.

[4] Fuzhou Institute of Oceanography, Minjiang University, Fuzhou 350108, China.

* Correspondence: glin2150@163.com (G.L.); huakunz2017@fafu.edu.cn (H.Z.); wangzh@fafu.edu.cn (Z.W.).

[†] These authors contributed equally to this work.

Abstract

The Elongator complex is conserved in a wide range of species and plays crucial roles in diverse cellular processes. We have previously shown that the Elongator protein PoELp3 was involved in the asexual development, pathogenicity, and autophagy of the rice blast fungus. In this study, we further revealed that PoElp3 functions via tRNA-mediated protein integrity. Based on the phenotypic results that overexpression of two of the tRNAs, tK(UUU) and tQ(UUG), could rescue the defects in fungal growth, pathogenicity and response to rapamycin of Δ*Poelp3* strain, we performed TMT-based proteomic analysis, and showed that 386 proteins were down-regulated in Δ*Poelp3* strain compared with wild type strain Guy11. Transcriptional analysis demonstrated that regulation of the 386 proteins by PoElp3 was independent of transcription. Codon usage assays revealed an enrichment of Glutamine CAA-biased mRNA in the 386 proteins compared with the 70-15 genome. Functional assessment of these proteins suggested that some of them were involved in either fungal growth, conidial development, pathogenicity, or autophagy. Taken together, our results suggested that PoElp3 acts through the tRNA-mediated translational efficiency to regulate asexual development, pathogenicity, and autophagy in the rice blast fungus.

Key words: Elongator, tRNA, proteomics, transcription, translational efficiency, rice blast fungus

1. Introduction

Transfer RNAs (tRNAs) are central players in protein biosynthesis that decipher the genetic code of mRNA and add appropriate amino acids into the growing amino acid chain (Holley *et al.* 1965; Ma *et al.* 2021). The simple primary sequence of tRNAs determines that it could fold into a diverse structure in addition to the one with biological function. Therefore, the posttranscriptional modifications of tRNA are essential for the maturing, folding, degradation, and decoding efficiency (Sokołowski *et al.* 2018). The 5-methoxycarbonylmethyl- 2-thiouridine (mcm^5s^2) modification of tRNA at U_{34} is one of the best-studied modifications and is conserved in many species (Leidel *et al.* 2009; Sokołowski *et al.* 2018). The mcm^5s^2-modified tRNAs decipher the NAA type codons and wobble onto NAG. For example, the lysine, glutamine, and glutamic acid are encoded by either AAA, CAA, and GAA, or AAG, CAG, and GAG, respective. And a single eukaryotic tRNA ($tRNA^{Lys}{}_{UUU}$ (tK^{UUU}), $tRNA^{Glu}{}_{UUC}$ (tE^{UUC}), or $tRNA^{Gln}{}_{UUG}$ (tQ^{UUG})) with a U at position 34 can recognize both the NAA and NAG (wobble) codons (Dewez *et al.* 2008; Goffena *et al.* 2018). The Elongator complex is involved in the first step of mcm^5s^2 modification by transferring a carboxymethyl group to U_{34} at the C_5 position to form the 5-carboxymethyluridine (cm^5U) precursor (Selvadurai *et al.* 2014). Although Elongator complex was found to modify 11 U_{34}-carrying tRNA species, only tK^{UUU}, tE^{UUC}, and tQ^{UUG} were subsequently thiolated (S2) (Johansson *et al.* 2008).

Elp3 is the catalytic subunit of the Elongator complex, which was originally identified in *Saccharomyces cerevisiae* as a component of elongating RNA polymerase II (RNAPII) holoenzyme (Otero *et al.* 1999). Elp3 contains a Gcn5-related N-terminal histone acetyltransferase (HAT) domain (Winkler *et al.* 2002), which was reported to have the acetyltransferase activity on histone proteins and other proteins (Creppe *et al.* 2009; Miśkiewicz *et al.* 2011; Laguesse *et al.* 2017; Lin *et al.* 2019; Planelles-Herrero *et al.* 2022). However, the effect of Elp3 on histone acetylation could be altered in different organisms,

80 in suggestive of diverse regulatory mechanisms in different backgrounds. For
81 example, the H3K14ac level was significantly reduced in *S. cerevisiae*
82 (Wittschieben *et al.* 2000), *Fusarium graminearum* (Lee *et al.* 2014) and
83 *Beauveria bassiana* (Cai *et al.* 2022), but not in *Aspergillus fumigatus* (Zhang
84 *et al.* 2022) and *Pyricularia oryzae* (Zhang *et al.* 2021). Elp3 also possesses a
85 radical S-adenosylmethionine (SAM) domain, which is responsible for the
86 modification of wobble uridine residues in eukaryotic tRNA (Dauden *et al.* 2019;
87 Lin *et al.* 2019; Abbassi *et al.* 2020). Increasing evidence demonstrated that
88 overexpression of corresponding hypomodified tRNA could rescue the defects
89 caused by Elongator complex-associated s^2U_{34} deficiency in many organisms,
90 such as *S. cerevisiae* (Esberg *et al.* 2006; Nedialkova and Leidel 2015;
91 Tükenmez *et al.* 2015; Jaciuk *et al.* 2023), *Caenorhabditis elegans*
92 (Nedialkova and Leidel 2015), and *Aspergillus fumigatus* (Zhang *et al.* 2022).
93 In line with this, studies in different species demonstrated that both the SAM
94 and KAT domains are required for the modification of tRNA by Elp3 proteins
95 (Selvadurai *et al.* 2014; Zhang *et al.* 2022). These results further support a key
96 role of Elongator complex in maintaining the wobbling function of tRNA.
97 In *P. oryzae* (syn. *Magnaporthe orzyae*), causal agent of the destructive
98 blast disease, autophagy is crutial for diverse developmental processes,
99 particularly, the appressorial development (Liu *et al.* 2007; Wilson and Talbot
100 2009; He *et al.* 2018; Sun *et al.* 2018; Yin *et al.* 2019). We had previously
101 shown that the Elp3 homolog was required for the development and
102 pathogenicity in the rice blast fungus *P. oryzae*, probably by maintaining the
103 autophagy homeostasis (Zhang *et al.* 2021). In this study, we aim to
104 investigate whether PoElp3 is involved in the wobbling function of tRNA and
105 subsequently the proteomic integrity.
106
107 **2. Materials and methods**
108 **2.1. Manipulation of fungal strains**
109 The fungal strains were cultivated as described previously (Anjago *et al.* 2022).

110 In brief, all strains were grown at 28 ºC on complete medium (CM, containing
111 yeast extract 0.6%, casamino acid 0.6%, sucrose 1%, agar 2%). For
112 rapamycin inhibition assay, the strains were grown at 28 ºC on MM medium
113 supplemented with or without 1 μg/mL rapamycin (He *et al.* 2018). For all the
114 fungal growth assays, images were taken at 7 days after cultivation. All the
115 assays were performed in three independent biological experiments. For RNA
116 and DNA extraction, the strains were grown in CM broth for 3 days before
117 collection.

118 **2.2 Spray inoculation assay**

119 The spray inoculation assays were performed as previously described with
120 minor modification (Zhang *et al.* 2021). Conidial suspensions (5×10^4
121 conidia/mL in 0.025% Tween-20 solution) of each strain were used for spray
122 inoculation assay on 14-day-old TP309 rice seedlings. The challenged rice
123 seedlings were then cultivated under the conditions described previously
124 (Giraldo *et al.* 2013). The symptoms were recorded and scored as previously
125 described (Valent *et al.* 1991).

126 **2.3. Construction of tRNA overexpression strains**

127 For the identification of $tRNA^{Lys}{}_{UUU}$ (tK^{UUU}) and $tRNA^{Gln}{}_{UUG}$ (tQ^{UUG}), we search
128 the rice blast genome for the homologs of SPBTRNALYS.06 and
129 SPBTRNAGLN.02, respectively, from *Schizosaccharomyces pombe* (fission
130 yeast). The identified coding sequences of each tRNA were amplified using the
131 primers listed in Appendix A and inserted into the *Xho*I and *Hind*III sites of
132 pKNT-RP27, which was then introduced into the ΔPoelp3 mutant strain
133 through the PEG3350-meidiated protoplast transformation (Sweigard *et al.*
134 1998). The resulting transformants were selected on TB3 medium with 600
135 μg/mL G418 and further tested through PCR-based genotyping.

136 **2.4. Proteomics analysis**

137 The proteomic analysis was performed as previously described with some
138 modifications (Zhang *et al.* 2022). Tandem Mass Tags (TMT)-based
139 proteomics analysis was conducted by Jingjie PTM Bio (Hangzhou, China). 50

140 μg total protein of each sample was digested with trypsin for TMT labeling and
141 fraction. The LC-MS/MS analysis was performed using an Orbitrap Exploris™
142 480 mass spectrometer (Thermo Scientific™, USA). The MS raw data were
143 processed with Proteome Discoverer (v2.4.1.15) and searched against 70-15
144 reference genome (Dean *et al.* 2005).

145 **2.5. RNA-sequencing and data analysis**

146 The RNA-sequencing and data analysis were performed as described
147 previously (Xie *et al.* 2023). The total RNA of each sample was used for the
148 construction of the RNA-seq library as described previously (Zhong *et al.*
149 2019). The libraries were sequenced using the Illumina NovaSeq 6000 system.
150 Quality assessment of raw reads (RNA-seq) was conducted using FASTQC
151 v0.11.3 (www.bioinformatics. babraham.ac.uk/bugzilla/). Adapters were
152 removed from the raw reads using Trim_galore v3.1
153 (https://github.com/FelixKrueger/TrimGalore/). Then, the RNA-seq reads were
154 aligned to 70-15 reference genome (Dean *et al.* 2005) using RSEM v1.3.3 (Li
155 and Dewey 2011). The quantification of expression counts were conducted
156 with transcript per million (TPM).

157 **2.6. Statistical analysis**

158 Statistical analysis was conducted by R packages in the R studio (Version
159 1.4.1106) environment (Xie *et al.* 2023).

160

161 **3. Results**

162 **3.1. Overexpression of tRNA could rescue the defects in Δ*Poelp3* strain**

163 To test whether the overexpression of tRNA could complement the defects
164 showed in Δ*Poelp3* strain, we search in the rice blast fungal genome for genes
165 encoding tK^{UUU} and tQ^{UUG}, the two tRNA that could rescue the transcription
166 and histone acetylation defects, as well as other phenotypes caused by the
167 absence of Elongator when overexpressed (Esberg *et al.* 2006). We found that
168 both tRNAs have two coding genes, with tK^{UUU}-4 and tK^{UUU}-6 localized at chr4
169 and chr6, tQ^{UUG}-2 and tQ^{UUG}-4 localized at chr2 and chr4, respectively. The

170 coding sequence of the two copies of each tRNAs was highly conserved, while
171 the franking sequences were highly polymorphic (Appendix B). The four tRNA
172 coding genes were fused with the ribosomal protein promoter (*RP27p*) and
173 introduced into the Δ*PoElp3* strain, respectively. At 7 days post inoculation, the
174 diameter of transfromants carrying the *RP27p* :: tK^{UUU} (herein after referred to
175 as '*tK(UUU)*') or *RP27p* :: tQ^{UUG} (herein after referred to as '*tQ(UUG)*') was
176 about 95%-100% of that of wild type, while the diameter of Δ*PoElp3* strain was
177 about 85% of that of the wild type (Fig. 1-A and B). Upon the treatment of
178 rapamycin, inhibitor of the Target-of-Rapamycin (TOR) signaling pathway, the
179 inhibition rate of fungal growth in the tK^{UUU} and tQ^{UUG} strains was reduced
180 compared to Δ*PoElp3* strain, but was still larger than that of Guy11 (Fig. 1-A
181 and C). Spray inoculation results showed that expression of tK^{UUU} and tQ^{UUG}
182 could also partially rescue the defects in pathogencity caused by the absence
183 of *PoELP3* (Fig. 1-D and E). These results suggested that the defects caused
184 by the deletion of *PoELP3* were at least partially caused by the inefficiency in
185 protein biosynthesis.
186

187 **3.2. PoElp3 is involved in the proper expression of protein**

188 To further investigate how PoElp3 regulates fungal development, pathogenicity,
189 and autophagy by affecting protein biosynthesis efficiency, we compared the
190 protein abundance between Δ*PoElp3* strain and the Guy11 wild type strain
191 through the tandem mass tags (TMT)-based quantitative proteomic analysis.
192 Among the 5,165 proteins identified and quantified in our proteomic data, 386
193 proteins were significantly down-regulated [fold change (FC) > 1/1.3 (*p-value* <
194 0.05)], and 403 proteins were up-regulated [FC < 1.3 (*p-value* < 0.05)] (Fig. 2-A
195 and B; Appendix C and D). The volcano plot result showed that most of the
196 differentially accumulated proteins (DAPs) with a FC ranged from 1.3 to 2.0,
197 and only a few of them with a FC >2.0 (Fig. 2-B). The clustering result showed
198 that the DAPs could be divided into different groups according to their
199 differential abundance between Guy11 and Δ*PoElp3* strain (Fig. 2-C).

200 **3.3. The DAPs involved in different pathways**

201 To perform functional classification of the DAPs, we divided the DAPs into 4
202 Categories: Q1 with a FC<1/1.5, Q2 with a FC between 1/1.5 to 1/1.3, Q3 with
203 a FC between 1.3 to 1.5, and Q4 with a FC>1.5 (Fig. 3-A). KEGG enrichment
204 results showed that the Q1 DAPs were enriched in pathways such as
205 Glyoxylate and dicarboxylate metabolism, biosynthesis of unsaturated fatty
206 acids, various types of N-glcan biosynthesis, sulfur metabolism and
207 sphingolipid metabolism. The Q2 DAPs were mainly enriched in steroid
208 biosynthesis, tryptophan metabolism, and terpenoid backbone biosynthesis.
209 While the Q3 and Q4 DAPs were mainly enriched in pathways such as
210 aminoacyl-tRNA biosynthesis, biosynthesis, and metabolism of amino acids
211 (Fig. 3-B). Protein domain enrichment showed that the Q1 DAPs were mainly
212 enriched in pathways such as adenylysulphate kinase, fatty acid desaturase,
213 and pyridine nucleotide-disulphide oxidoreductase. The Q2 DAPs were mainly
214 enriched in pathways such as dynamin, flavodoxin, enoyl-(axyl carrier protein)
215 reductase, and alpha amylase. While the Q3 and Q4 DAPs were mainly
216 enriched in pathways such as tRNA synthetases, pyridoxamine 5'-phosphate
217 oxidase, NADH oxidase and oxidoreductase NAD-binding domain (Fig. 3-C).

218

219 **3.4. PoElp3 regulated the accumulation of proteins independent of**
220 **transcription**

221 To further assess whether the DAPs were associated with the differential
222 transcription level of their coding genes, we performed a comparative
223 transcriptome analysis between the wild type and Δ*Poelp3* strains. We showed
224 that only 535 genes were down-regulated, and 1,049 genes were up-regulated
225 in Δ*Poelp3* compared with the wild type strain Guy11 (Fig. 4-A). We further
226 investigated the transcription level of DAPs down-regulated in Δ*Poelp3* strain,
227 and found that, among the 386 proteins down-regulated in Δ*Poelp3* strain, only
228 19 and 25 of them showing either higher or lower transcription level in the
229 mutant strain (Fig. 4-B; Appendix E). While among the 403 DAPs up-regulated

230 in Δ*Poelp3* strain, only 22 showing lower transcription level in the mutant strain,
231 but 138 showing higher transcription level in the mutant strain (Appendix F),
232 which could be affected indirectly. Taken together, these results suggested that
233 the protein level of most of the DAPs in Δ*Poelp3* strain was independent of the
234 transcription level.
235

236 **3.5. Enrichment of Glutamine CAA-biased mRNA in the DAPs**
237 **down-regulated in Δ*Poelp3* strain**

238 To test whether there is a bias toward the use of NAA codons, we first
239 surveyed the coding sequence of 70-15 genome (whole genome, WG), and
240 found that 65.0%, 52.5% and 58.0% of the coding sequences showed an
241 NAA:NAG ratio > 1 for Lysine, Glutamine, and Glutamic acid, respectively
242 (Table 1). We then surveyed the coding sequence of DAPs down-regulated in
243 Δ*Poelp3* strain. Since the DAPs down-regulated in Δ*Poelp3* strain were
244 supposed to be caused by the absence of PoElp3, and are therefore referred
245 to as PoElp3 regulated protein candidates (Erps) hereafter. We found that
246 58.8.0%, 64.8% and 50.5.0% of the coding sequences showed an NAA:NAG
247 ratio > 1 for Lysine, Glutamine, and Glutamic acid, respectively (Table 1;
248 Appendix G). These results suggested an enrichment of Glutamine
249 CAA-biased mRNA in the Erps compared with 70-15 genome.
250

251 **3.6. The Elp3-regulated proteins involved in asexual development and**
252 **pathogenicity**

253 To assess whether any of the DAPs down-regulated in Δ*Poelp3* strain
254 functions similarly to PoElp3, we searched in the PubMed database for
255 publications associated with the 386 DAPs and found six DAPs involved in
256 vegetative growth, conidiation, pathogenicity and/or autophagy. These DAPs
257 presented a Fold Change (FC) ranging from 0.49~0.76, and their transcription
258 level in Δ*Poelp3* strain was no less than that in Wild type strain Guy11 (Table 2
259 and Appendix E). Among them, *ERP1* encodes a core protein of ESCRT-III

260 subcomplex (Snf7) involved in asexual development, pathogenicity and
261 autophagy (Cheng *et al.* 2018). *ERP2* encoding a Rho3 homolog is involved in
262 appressorial development and pathogenicity (Zheng *et al.* 2007). *ERP3*
263 encodes an ADP-ribosylation factor 6 protein (Arf6), which is involved in
264 endocytosis and polarity during the asexual development (Zhu *et al.* 2016).
265 *ERP4* encodes a tetrahydroxynaphthalene reductase (Buf1) and is required for
266 melanin biosynthesis and full virulence (Zhu *et al.* 2021). *ERP5* encodes an
267 amidophosphoribosyltransferase (Ade4), which catalyzes the conversion of
268 5-phosphoribosyl-1-pyrophosphate into 5-phosphoribosyl-1-amine in the de
269 novo purine biosynthetic pathway and is required for conidiation and
270 pathogenicity (Aron *et al.* 2022). *ERP6* encoding a glyoxylate
271 aminotransferase 1 (Agt1) is required for mobilization and utilization of
272 triglycerides during infection (Bhadauria *et al.* 2012a; Bhadauria *et al.* 2012b).
273 Besides, we also found DAPs with their homologs in other fungal species
274 associated with development or pathogenicity. For example, the MGG_03393
275 encodes a secondary metabolism regulator (Lae1) and is involved in asexual
276 development and mycoparasitism of *Trichoderma atroviride* (Karimi Aghcheh
277 *et al.* 2013). MGG_00413T0 encoding a putative β-1,3-glucanosyltransferase
278 (Gel7) is required for the cell wall integrity under stress conditions (Zhao *et al.*
279 2014).
280

281 **4. Discussion**

282 The Elongator complex is conserved among different species and increasing
283 evidence demonstrated that they function mainly through the modification of
284 tRNA (Bauer *et al.* 2012; Candiracci *et al.* 2019; Dauden *et al.* 2019). In
285 supporting this, overexpression of unmodified tRNA for glutamine, glutamic
286 acid and lysine was efficient to restore the defects caused by the absence of
287 Elongator in several studies (Esberg *et al.* 2006; Bauer *et al.* 2012; Zhang *et al.*
288 2022), probably by increasing the intracellular concentration of tRNAs to
289 compensate for decreased binding affinity in the Elongator mutants (Esberg *et*

290 *al.* 2006; Nedialkova and Leidel 2015; Tükenmez *et al.* 2015; Sokołowski *et al.*
291 2018). In this study, the phenotypic analysis showed that overexpression of
292 *tK*(*UUU*) or *tQ*(*UUG*) could rescue fully the defects in fungal growth, and
293 partially the defects in pathogenicity and response to rapamycin caused by the
294 deletion of *PoELP3*, which indicated that PoElp3 may act through the
295 tRNA-mediated protein integrity to regulate the fungal growth in rice blast
296 fungus (Zhang *et al.* 2021).

297 Elp3 proteins had been proved to catalyze the modification of tRNA at
298 wobbling U34 and consequently maintain the translation efficiency of proteins
299 encoded by tK(UUU), tE(UUC), or tQ(UUG) (Bauer *et al.* 2012; Goffena *et al.*
300 2018). Previous studies suggested that NAA-biased codon usage is not
301 always necessary for the Elongator regulated protein integraty via the tRNA
302 modification. For example, the biased codon usage was exhibited in in yeast
303 (Bauer *et al.* 2012), but not in *A. fumigatus* (Zhang *et al.* 2022). In this study,
304 we showed that the Erps displayed an enrichment of Glutamine CAA-biased
305 -biased mRNA, which suggested that different regulatory mechanisms might
306 be applied in the Elp3 regulated translational efficiency.

307 The Elongator proteins could act by regulating the translational
308 efficiency of target with important functions. For example, in fission yeast, the
309 Elongator controls cell division by regulating the translational efficiency of the
310 Cdr2 kinase (Bauer *et al.* 2012). Our functional assessment of the Erps
311 showed that some of them were associated with asexual development, such
312 as Erp1/Snf7, Erp2/Rho3, Erp3/ArF6, Erp4/Ade4, Erp5/Buf1, Erp6/Agt1, Lae1
313 and Gel7. Recent study in *A. fumigatus* showed that defects in development
314 and pathogenicity in Δ*elp3* strain could be caused by the amino acid
315 homeostasis imbalance (Zhang *et al.* 2022). We also found that many Erps
316 were involved in the biosynthesis and metabolism of amino acids, suggesting a
317 role of PoElp3 in development and pathogenicity by modulating amino acid
318 homeostasis. Moreover, we also found Erps that may be involved in autophagy
319 through different mechanisms. For example, Erp1/Snf7 acts in vesicle

320 trafficking and autophagy (Cheng *et al.* 2018). Erp3/Arf6 is involved in
321 autophagy homeostasis through the generation of phosphatidylinositol
322 4,5-bisphosphate (PIP(2)) and induction of phospholipase D (PLD) activity
323 (Moreau *et al.* 2012). The absence of Erp4/Ade4 caused delayed glycogen
324 mobilization and reduced turgor pressure in the appressoria (Aron *et al.* 2022),
325 the representative cellular processes of autophagy during appressorial
326 development in rice blast fungus (Deng *et al.* 2008; Kershaw and Talbot 2009).
327 Besides, we also found that some Erps were involved in the sphingolipid
328 metabolism pathway. Although the role of sphingolipid was not well studied in
329 filamentous fungus (Liu *et al.* 2019), it was shown to be involved in autophagy
330 homeostasis in mammals (Li *et al.* 2014). These results together suggested
331 that PoElp3 is required for the development, pathogenicity and autophagy by
332 regulating the translational efficiency of proteins involved in diverse pathways.
333 And detailed analysis of the Erps may further support the function of PoElp3 in
334 autophagy via the tRNA-mediated protein integrity.

335 Although the role of Elongator in tRNA-mediated protein integrity is well
336 established, there are several lines of evidence suggesting that Elp3 also acts
337 by acetylation of other proteins, such as microtubules (Planelles-Herrero *et al.*
338 2022), α-tubulin (Creppe *et al.* 2009), bruchpilot (Laguesse *et al.* 2017), and
339 connexin-43 (Miśkiewicz *et al.* 2011) in animal cells. In this study, we also
340 found that overexpression of the two tRNAs could only partially rescue the
341 response of Δ*Poelp3* to rapamycin treatment. Similar results were also
342 reported in previous studies performed in fission yeast (Bauer *et al.* 2012) and
343 *A. fumigatus* (Zhang *et al.* 2022). And these results together suggested that
344 Elp3 may also act through other pathway(s).

345

346 **5. Conclusion**

347 In conclusion, our results demonstrated that PoElp3 was involved in the
348 asexual development, pathogenicity, and autophagy by regulating the
349 tRNA-mediated protein integrity.

Competing interests

The authors declare that they have no competing interests.

References

Abbassi NE, Biela A, Glatt S and Lin TY. 2020. How Elongator Acetylates tRNA Bases. *Int J Mol Sci,* **21,**

Anjago WM, Biregeya J, Shi M, Chen Y, Wang Y, Wang Z, Hong Y and Chen M. 2022. The calcium chloride responsive type 2C protein phosphatases play synergistic roles in regulating MAPK pathways in *Magnaporthe oryzae*. *J Fungi (Basel),* **8,**

Aron O, Otieno FJ, Tijjani I, Yang Z, Xu H, Weng S, Guo J, Lu S, Wang Z and Tang W. 2022. De novo purine nucleotide biosynthesis mediated by MoAde4 is required for conidiation, host colonization and pathogenicity in *Magnaporthe oryzae*. *Appl Microbiol Biotechnol,* **106,** 5587-5602.

Bauer F, Matsuyama A, Candiracci J, Dieu M, Scheliga J, Wolf DA, Yoshida M and Hermand D. 2012. Translational control of cell division by Elongator. *Cell Rep,* **1,** 424-433.

Bhadauria V, Banniza S, Vandenberg A, Selvaraj G and Wei Y. 2012a. Alanine: Glyoxylate aminotransferase 1 is required for mobilization and utilization of triglycerides during infection process of the rice blast pathogen, *Magnaporthe oryzae*. *Plant Signal Behav,* **7,** 1206-1208.

Bhadauria V, Banniza S, Vandenberg A, Selvaraj G and Wei Y. 2012b. Peroxisomal alanine: glyoxylate aminotransferase AGT1 is indispensable for appressorium function of the rice blast pathogen, *Magnaporthe oryzae*. *PLoS One,* **7,** e36266.

Cai Q, Wang J, Xie J, Jiang D and Keyhani NO. 2022. The Elongator subunit Elp3 regulates development, stress tolerance, cell cycle, and virulence in the entomopathogenic fungus *Beauveria bassiana*. *J Fungi (Basel),* **8,**

Candiracci J, Migeot V, Chionh YH, Bauer F, Brochier T, Russell B, Shiozaki K, Dedon P and Hermand D. 2019. Reciprocal regulation of TORC signaling and tRNA modifications by Elongator enforces nutrient-dependent cell fate. *Sci Adv,* **5,** eaav0184.

Cheng J, Yin Z, Zhang Z and Liang Y. 2018. Functional analysis of MoSnf7 in *Magnaporthe oryzae*. *Fungal Genet Biol,* **121,** 29-45.

Creppe C, Malinouskaya L, Volvert ML, Gillard M, Close P, Malaise O, Laguesse S, Cornez I, Rahmouni S, Ormenese S, Belachew S, Malgrange B, Chapelle JP, Siebenlist U, Moonen G, Chariot A and Nguyen L. 2009. Elongator controls the migration and differentiation of cortical neurons

through acetylation of alpha-tubulin. *Cell,* **136,** 551-564.

Dauden MI, Jaciuk M, Weis F, Lin TY, Kleindienst C, Abbassi NEH, Khatter H, Krutyhołowa R, Breunig KD, Kosinski J, Müller CW and Glatt S. 2019. Molecular basis of tRNA recognition by the Elongator complex. *Sci Adv,* **5,** eaaw2326.

Dean RA, Talbot NJ, Ebbole DJ, Farman ML, Mitchell TK, Orbach MJ, Thon M, Kulkarni R, Xu JR, Pan H, Read ND, Lee YH, Carbone I, Brown D, Oh YY, Donofrio N, Jeong JS, Soanes DM, Djonovic S, Kolomiets E, Rehmeyer C, Li W, Harding M, Kim S, Lebrun MH, Bohnert H, Coughlan S, Butler J, Calvo S, Ma LJ, Nicol R, Purcell S, Nusbaum C, Galagan JE and Birren BW. 2005. The genome sequence of the rice blast fungus *Magnaporthe grisea*. *Nature,* **434,** 980-986.

Deng YZ, Ramos-Pamplona M and Naqvi NI. 2008. Methods for functional analysis of macroautophagy in filamentous fungi. *Methods Enzymol,* **451,** 295-310.

Dewez M, Bauer F, Dieu M, Raes M, Vandenhaute J and Hermand D. 2008. The conserved Wobble uridine tRNA thiolase Ctu1-Ctu2 is required to maintain genome integrity. *Proc Natl Acad Sci U S A,* **105,** 5459-5464.

Esberg A, Huang B, Johansson MJ and Byström AS. 2006. Elevated levels of two tRNA species bypass the requirement for elongator complex in transcription and exocytosis. *Mol Cell,* **24,** 139-148.

Giraldo MC, Dagdas YF, Gupta YK, Mentlak TA, Yi M, Martinez-Rocha AL, Saitoh H, Terauchi R, Talbot NJ and Valent B. 2013. Two distinct secretion systems facilitate tissue invasion by the rice blast fungus *Magnaporthe oryzae*. *Nat Commun,* **4,** 1996.

Goffena J, Lefcort F, Zhang Y, Lehrmann E, Chaverra M, Felig J, Walters J, Buksch R, Becker KG and George L. 2018. Elongator and codon bias regulate protein levels in mammalian peripheral neurons. *Nat Commun,* **9,** 889.

He M, Xu Y, Chen J, Luo Y, Lv Y, Su J, Kershaw MJ, Li W, Wang J, Yin J, Zhu X, Liu X, Chern M, Ma B, Wang J, Qin P, Chen W, Wang Y, Wang W, Ren Z, Wu X, Li P, Li S, Peng Y, Lin F, Talbot NJ and Chen X. 2018. MoSnt2-dependent deacetylation of histone H3 mediates MoTor-dependent autophagy and plant infection by the rice blast fungus *Magnaporthe oryzae*. *Autophagy,* **14,** 1543-1561.

Holley RW, Apgar J, Everett GA, Madison JT, Marquisee M, Merrill SH, Penswick JR and Zamir A. 1965. STRUCTURE OF A RIBONUCLEIC ACID. *Science,* **147,** 1462-1465.

Jaciuk M, Scherf D, Kaszuba K, Gaik M, Rau A, Kościelniak A, Krutyhołowa R, Rawski M, Indyka P, Graziadei A, Chramiec-Głąbik A, Biela A, Dobosz D, Lin TY, Abbassi NE, Hammermeister A, Rappsilber J, Kosinski J, Schaffrath R and Glatt S. 2023. Cryo-EM structure of the fully assembled Elongator complex. *Nucleic Acids Res,* **51,** 2011-2032.

Johansson MJ, Esberg A, Huang B, Björk GR and Byström AS. 2008. Eukaryotic wobble uridine

415 modifications promote a functionally redundant decoding system. *Mol Cell Biol,* **28,**
416 3301-3312.

417 Karimi Aghcheh R, Druzhinina IS and Kubicek CP. 2013. The putative protein methyltransferase LAE1 of
418 Trichoderma atroviride is a key regulator of asexual development and mycoparasitism. *PLoS*
419 *One,* **8,** e67144.

420 Kershaw MJ and Talbot NJ. 2009. Genome-wide functional analysis reveals that infection-associated
421 fungal autophagy is necessary for rice blast disease. *Proc Natl Acad Sci U S A,* **106,**
422 15967-15972.

423 Laguesse S, Close P, Van Hees L, Chariot A, Malgrange B and Nguyen L. 2017. Loss of Elp3 impairs the
424 acetylation and distribution of connexin-43 in the developing cerebral cortex. *Front Cell*
425 *Neurosci,* **11,** 122.

426 Lee Y, Min K, Son H, Park AR, Kim JC, Choi GJ and Lee YW. 2014. ELP3 is involved in sexual and asexual
427 development, virulence, and the oxidative stress response in *Fusarium graminearum*. *Mol*
428 *Plant Microbe Interact,* **27,** 1344-1355.

429 Leidel S, Pedrioli PG, Bucher T, Brost R, Costanzo M, Schmidt A, Aebersold R, Boone C, Hofmann K and
430 Peter M. 2009. Ubiquitin-related modifier Urm1 acts as a sulphur carrier in thiolation of
431 eukaryotic transfer RNA. *Nature,* **458,** 228-232.

432 Li B and Dewey CN. 2011. RSEM: accurate transcript quantification from RNA-Seq data with or without
433 a reference genome. *BMC Bioinformatics,* **12,** 323.

434 Li Y, Li S, Qin X, Hou W, Dong H, Yao L and Xiong L. 2014. The pleiotropic roles of sphingolipid signaling
435 in autophagy. *Cell Death Dis,* **5,** e1245.

436 Lin TY, Abbassi NEH, Zakrzewski K, Chramiec-Głąbik A, Jemioła-Rzemińska M, Różycki J and Glatt S.
437 2019. The Elongator subunit Elp3 is a non-canonical tRNA acetyltransferase. *Nat Commun,* **10,**
438 625.

439 Liu XH, Liang S, Wei YY, Zhu XM, Li L, Liu PP, Zheng QX, Zhou HN, Zhang Y, Mao LJ, Fernandes CM, Del
440 Poeta M, Naqvi NI and Lin FC. 2019. Metabolomics analysis identifies sphingolipids as key
441 signaling moieties in appressorium morphogenesis and function in *Magnaporthe oryzae*.
442 *mBio,* **10,**

443 Liu XH, Lu JP, Zhang L, Dong B, Min H and Lin FC. 2007. Involvement of a *Magnaporthe grisea*
444 serine/threonine kinase gene, MgATG1, in appressorium turgor and pathogenesis. *Eukaryot*
445 *Cell,* **6,** 997-1005.

446 Ma X, Liu C and Cao X. 2021. Plant transfer RNA-derived fragments: Biogenesis and functions. *J Integr*
447 *Plant Biol,* **63,** 1399-1409.

448 Miśkiewicz K, Jose LE, Bento-Abreu A, Fislage M, Taes I, Kasprowicz J, Swerts J, Sigrist S, Versées W,
449 Robberecht W and Verstreken P. 2011. ELP3 controls active zone morphology by acetylating
450 the ELKS family member Bruchpilot. *Neuron,* **72,** 776-788.
451 Moreau K, Ravikumar B, Puri C and Rubinsztein DC. 2012. Arf6 promotes autophagosome formation
452 via effects on phosphatidylinositol 4,5-bisphosphate and phospholipase D. *J Cell Biol,* **196,**
453 483-496.
454 Nedialkova DD and Leidel SA. 2015. Optimization of codon translation rates via tRNA modifications
455 maintains proteome integrity. *Cell,* **161,** 1606-1618.
456 Otero G, Fellows J, Li Y, de Bizemont T, Dirac AM, Gustafsson CM, Erdjument-Bromage H, Tempst P and
457 Svejstrup JQ. 1999. Elongator, a multisubunit component of a novel RNA polymerase II
458 holoenzyme for transcriptional elongation. *Mol Cell,* **3,** 109-118.
459 Planelles-Herrero VJ, Bittleston A, Seum C, Daeden A, Gaitan MG and Derivery E. 2022. Elongator
460 stabilizes microtubules to control central spindle asymmetry and polarized trafficking of cell
461 fate determinants. *Nat Cell Biol,* **24,** 1606-1616.
462 Selvadurai K, Wang P, Seimetz J and Huang RH. 2014. Archaeal Elp3 catalyzes tRNA wobble uridine
463 modification at C5 via a radical mechanism. *Nat Chem Biol,* **10,** 810-812.
464 Sokołowski M, Klassen R, Bruch A, Schaffrath R and Glatt S. 2018. Cooperativity between different
465 tRNA modifications and their modification pathways. *Biochim Biophys Acta Gene Regul Mech,*
466 **1861,** 409-418.
467 Sun G, Elowsky C, Li G and Wilson RA. 2018. TOR-autophagy branch signaling via Imp1 dictates
468 plant-microbe biotrophic interface longevity. *PLoS Genet,* **14,** e1007814.
469 Sweigard JA, Carroll AM, Farrall L, Chumley FG and Valent B. 1998. *Magnaporthe grisea* pathogenicity
470 genes obtained through insertional mutagenesis. *Mol Plant Microbe Interact,* **11,** 404-412.
471 Tükenmez H, Xu H, Esberg A and Byström AS. 2015. The role of wobble uridine modifications in +1
472 translational frameshifting in eukaryotes. *Nucleic Acids Res,* **43,** 9489-9499.
473 Valent B, Farrall L and Chumley FG. 1991. *Magnaporthe grisea* genes for pathogenicity and virulence
474 identified through a series of backcrosses. *Genetics,* **127,** 87-101.
475 Wilson RA and Talbot NJ. 2009. Under pressure: investigating the biology of plant infection by
476 *Magnaporthe oryzae*. *Nat Rev Microbiol,* **7,** 185-195.
477 Winkler GS, Kristjuhan A, Erdjument-Bromage H, Tempst P and Svejstrup JQ. 2002. Elongator is a
478 histone H3 and H4 acetyltransferase important for normal histone acetylation levels *in vivo*.

479 *Proc Natl Acad Sci U S A,* **99,** 3517-3522.

480 Wittschieben BO, Fellows J, Du W, Stillman DJ and Svejstrup JQ. 2000. Overlapping roles for the
481 histone acetyltransferase activities of SAGA and elongator *in vivo*. *Embo j,* **19,** 3060-3068.

482 Xie J, Tang W, Lu G, Hong Y, Zhong Z, Wang Z and Zheng H. 2023. Histone H3K27me3 methylation
483 regulates the expression of secreted proteins distributed at fast-evolving regions through
484 transcriptional repression of transposable elements. *Journal of Integrative Agriculture,*

485 Yin Z, Chen C, Yang J, Feng W, Liu X, Zuo R, Wang J, Yang L, Zhong K, Gao C, Zhang H, Zheng X, Wang P
486 and Zhang Z. 2019. Histone acetyltransferase MoHat1 acetylates autophagy-related proteins
487 MoAtg3 and MoAtg9 to orchestrate functional appressorium formation and pathogenicity in
488 *Magnaporthe oryzae*. *Autophagy,* **15,** 1234-1257.

489 Zhang L, Chen S, Qi M, Cao X, Liang N, Li Q, Tang W, Lu G, Zhou J, Yu W, Wang Z and Zheng H. 2021.
490 The putative elongator complex protein Elp3 is involved in asexual development and
491 pathogenicity by regulating autophagy in the rice blast fungus. *Journal of Integrative*
492 *Agriculture,* **20,** 2944-2956.

493 Zhang Y, Wang Y, Fan J, Zhu G and Lu L. 2022. *Aspergillus fumigatus* Elongator complex subunit 3
494 affects hyphal growth, adhesion and virulence through wobble uridine tRNA modification.
495 *PLoS Pathog,* **18,**

496 Zhao W, Li C, Liang J and Sun S. 2014. The *Aspergillus fumigatus* β-1,3-glucanosyltransferase Gel7 plays
497 a compensatory role in maintaining cell wall integrity under stress conditions. *Glycobiology,*
498 **24,** 418-427.

499 Zheng W, Chen J, Liu W, Zheng S, Zhou J, Lu G and Wang Z. 2007. A Rho3 homolog is essential for
500 appressorium development and pathogenicity of *Magnaporthe grisea*. *Eukaryot Cell,* **6,**
501 2240-2250.

502 Zhong Z, Lin L, Chen M, Lin L, Chen X, Lin Y, Chen X, Wang Z, Norvienyeku J and Zheng H. 2019.
503 Expression Divergence as an evolutionary alternative mechanism adopted by two rice
504 subspecies against rice blast infection. *Rice (N Y),* **12,** 12.

505 Zhu S, Yan Y, Qu Y, Wang J, Feng X, Liu X, Lin F and Lu J. 2021. Role refinement of melanin synthesis
506 genes by gene knockout reveals their functional diversity in *Pyricularia oryzae strains*.
507 *Microbiol Res,* **242,** 126620.

508 Zhu X, Zhou T, Chen L, Zheng S, Chen S, Zhang D, Li G and Wang Z. 2016. Arf6 controls endocytosis and
509 polarity during asexual development of *Magnaporthe oryzae*. *FEMS Microbiol Lett,* **363,**

510

511 ## Figure legends

512 **Fig. 1** Overexpression of *tK*(*UUU*) or *tQ*(*UUG*) could partially rescue the
513 defects in Δ*Poelp3* strain. A, the indicated strains grown on CM, MM and MM
514 supplemented with 1 μg/uL rapamycin (MM+Rap). B, colony diameter of
515 indicated strains grown on CM. C, the inhibition rate of indicated strains upon
516 the treatment of 1 μg/uL rapamycin. The letters indicate statistically significant
517 differences ($p<0.01$). D, leaves of rice cultivar TP309 were sprayed with
518 conidial suspensions (5×10^4conidia mL^{-1}) of strains indicated. E, quantification
519 of different lesion types. Data were shown as the mean±SE (n=3).
520 **Fig. 2** The differentially accumulated proteins (DAPs) between Δ*Poelp3* and
521 Guy11 strains. A, quantitative identification of proteins upregulated and
522 downregulated in Δ*Poelp3* strain though TMT. B, volcano plot showing the fold
523 change of the differentially accumulated proteins. C, cluster analysis of the
524 DAPs.
525 **Fig. 3** Functional classification of the DAPs. A, the four Q Categories of the
526 DAPs. B, classification of DAPs according to the KEGG pathway. C,
527 classification of DAPs according to protein domain.
528 **Fig. 4** Comparative transcriptional analysis between wild type and Δ*Poelp3*
529 strains. A, differentially expressed genes between wild type and Δ*Poelp3*
530 strains. B, comparative analysis of the transcription level of DAPs
531 down-regulated in Δ*Poelp3* strain.
532 **Table 1** Codon usage of lysine, glutamine and glutamic acid in the Erps.
533 **Table 2** The *ERPs* functionally studied in *P. oryzae*
534
535 **Supporting information**
536 **Appendix A.** Primers used in this study.
537 **Appendix B.** Alignment of tRNAs from *Schizosaccharomyces pombe* (fission
538 yeast) and *P. oryzae*.
539 **Appendix C.** Proteins up-regulated in Δ*Poelp3* strain.
540 **Appendix D.** Proteins down-regulated in Δ*Poelp3* strain.
541 **Appendix E.** The transcription level of DAPs down-regulated in Δ*Poelp3*

542 strain.

543 **Appendix F.** Comparative analysis of the transcription level of DAPs

544 up-regulated in Δ*Poelp3* strain.

545 **Appendix G.** Codons used in Erps.

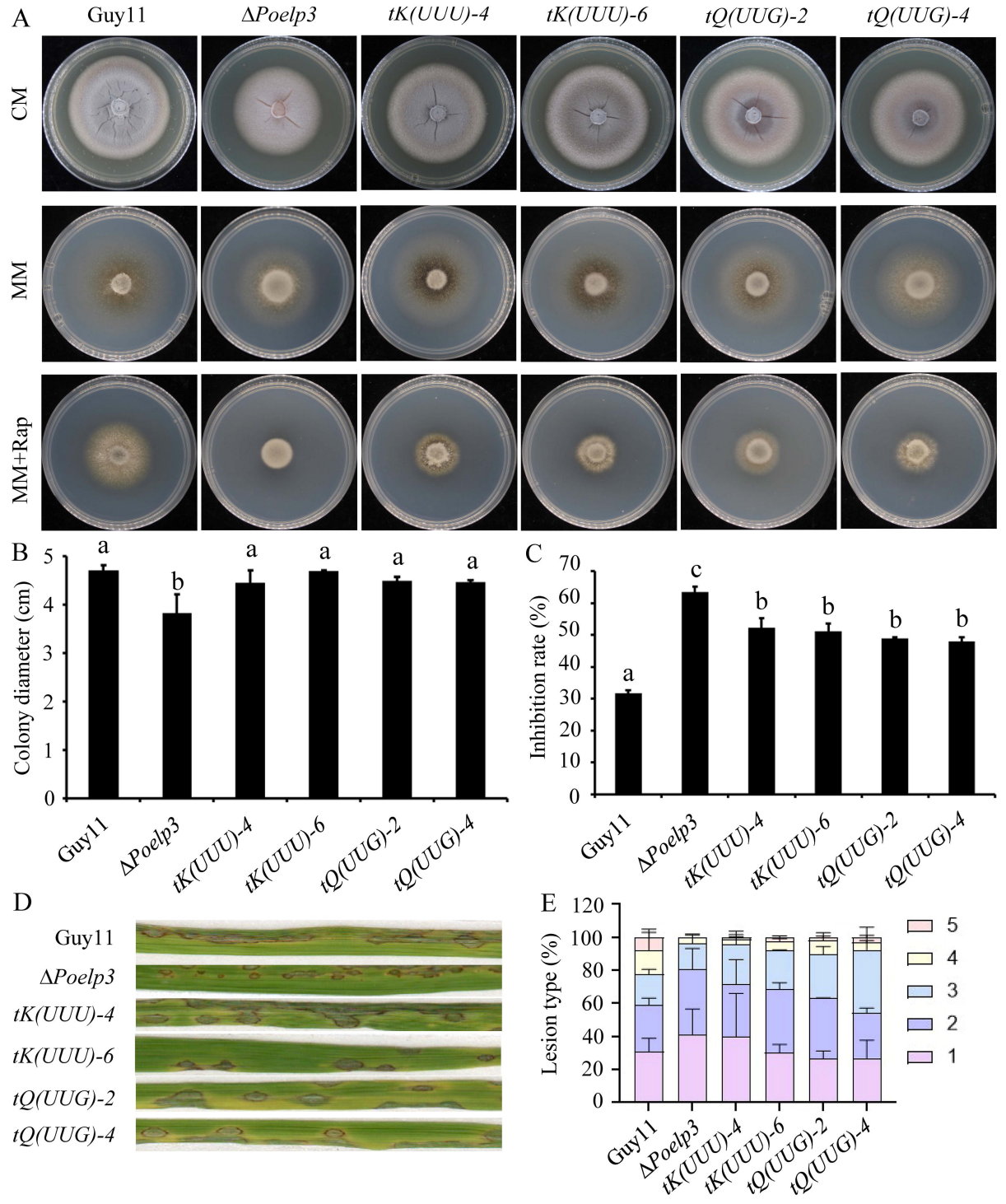
A
Guy11
ΔPoelp3
tK(UUU)-4
tK(UUU)-6
tQ(UUG)-2
tQ(UUG)-4
CM
MM
MM+Rap
B
Colony diameter (cm)
0
1
2
3
4
5
a
b
a
a
a
a
Guy11
ΔPoelp3
tK(UUU)-4
tK(UUU)-6
tQ(UUG)-2
tQ(UUG)-4
C
Inhibition rate (%)
0
10
20
30
40
50
60
70
a
c
b
b
b
b
Guy11
ΔPoelp3
tK(UUU)-4
tK(UUU)-6
tQ(UUG)-2
tQ(UUG)-4
D
Guy11
ΔPoelp3
tK(UUU)-4
tK(UUU)-6
tQ(UUG)-2
tQ(UUG)-4
E
Lesion type (%)
0
20
40
60
80
100
120
5
4
3
2
1
Guy11
ΔPoelp3
tK(UUU)-4
tK(UUU)-6
tQ(UUG)-2
tQ(UUG)-4

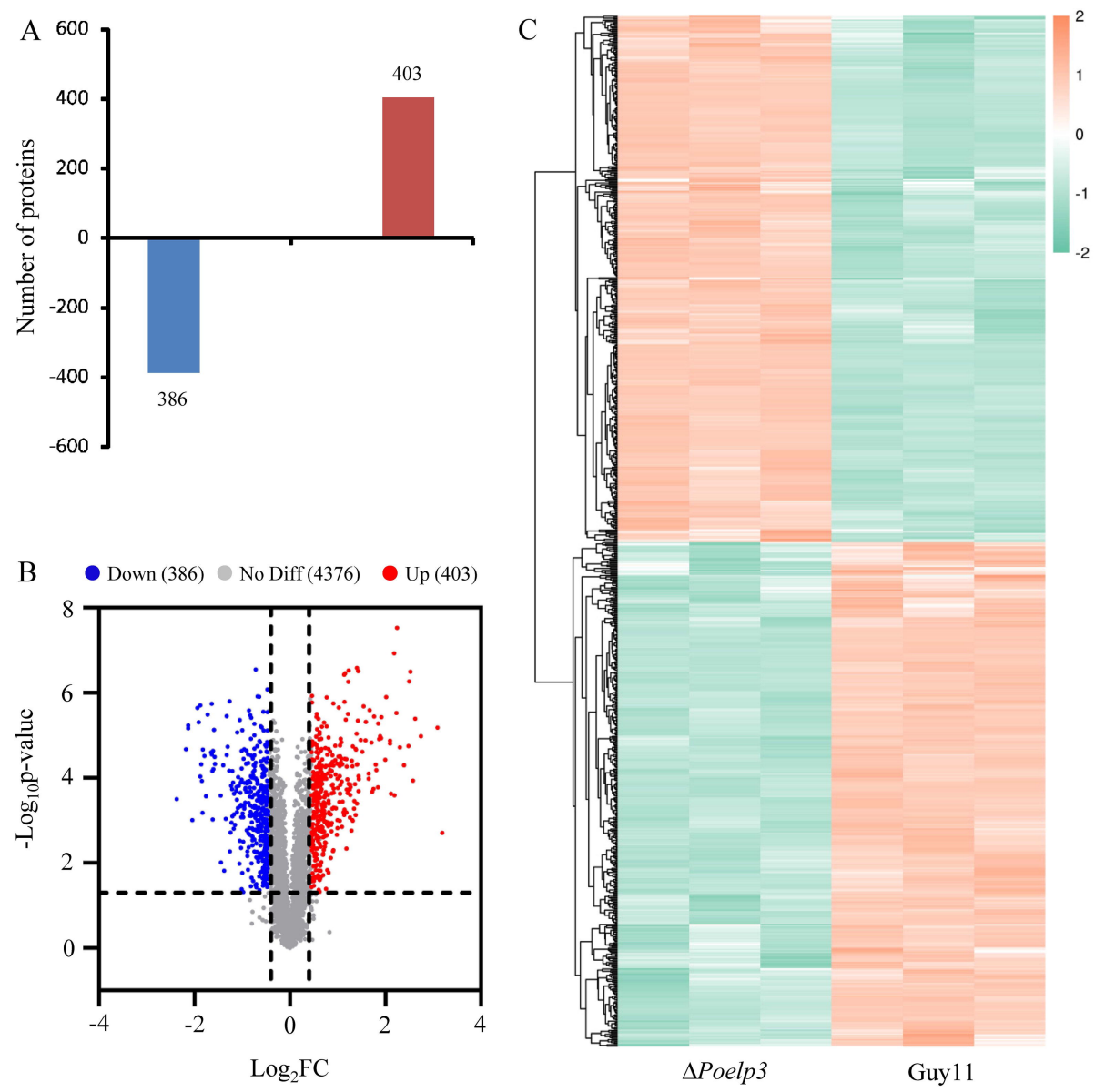
A
Number of proteins
600
400
200
0
-200
-400
-600
403
386
B
Down (386)
No Diff (4376)
Up (403)
-Log10p-value
8
6
4
2
0
-4
-2
0
2
4
Log2FC
C
2
1
0
-1
-2
ΔPoelp3
Guy11

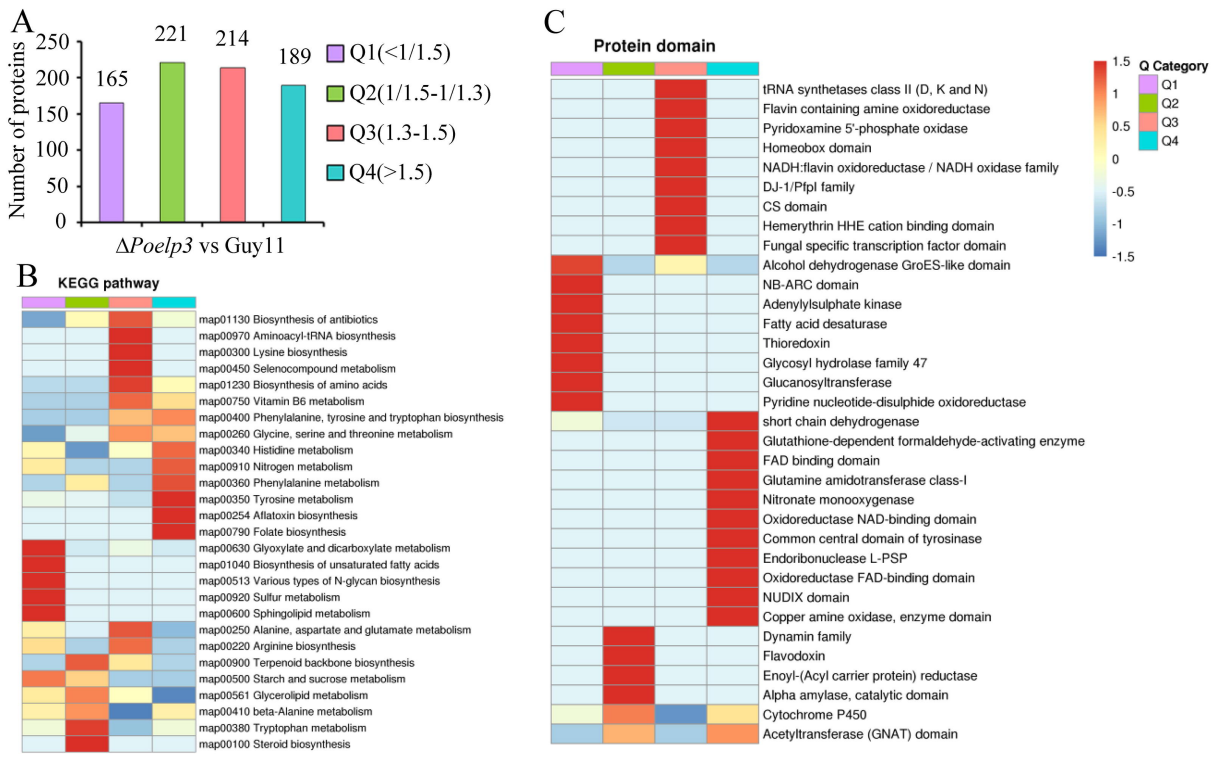
A
Number of proteins
250
200
150
100
50
0
165
221
214
189
Q1(<1/1.5)
Q2(1/1.5-1/1.3)
Q3(1.3-1.5)
Q4(>1.5)
ΔPoelp3 vs Guy11
B
KEGG pathway
map01130 Biosynthesis of antibiotics
map00970 Aminoacyl-tRNA biosynthesis
map00300 Lysine biosynthesis
map00450 Selenocompound metabolism
map01230 Biosynthesis of amino acids
map00750 Vitamin B6 metabolism
map00400 Phenylalanine, tyrosine and tryptophan biosynthesis
map00260 Glycine, serine and threonine metabolism
map00340 Histidine metabolism
map00910 Nitrogen metabolism
map00360 Phenylalanine metabolism
map00350 Tyrosine metabolism
map00254 Aflatoxin biosynthesis
map00790 Folate biosynthesis
map00630 Glyoxylate and dicarboxylate metabolism
map01040 Biosynthesis of unsaturated fatty acids
map00513 Various types of N-glycan biosynthesis
map00920 Sulfur metabolism
map00600 Sphingolipid metabolism
map00250 Alanine, aspartate and glutamate metabolism
map00220 Arginine biosynthesis
map00900 Terpenoid backbone biosynthesis
map00500 Starch and sucrose metabolism
map00561 Glycerolipid metabolism
map00410 beta-Alanine metabolism
map00380 Tryptophan metabolism
map00100 Steroid biosynthesis
C
Protein domain
tRNA synthetases class II (D, K and N)
Flavin containing amine oxidoreductase
Pyridoxamine 5'-phosphate oxidase
Homeobox domain
NADH:flavin oxidoreductase / NADH oxidase family
DJ-1/PfpI family
CS domain
Hemerythrin HHE cation binding domain
Fungal specific transcription factor domain
Alcohol dehydrogenase GroES-like domain
NB-ARC domain
Adenylylsulphate kinase
Fatty acid desaturase
Thioredoxin
Glycosyl hydrolase family 47
Glucanosyltransferase
Pyridine nucleotide-disulphide oxidoreductase
short chain dehydrogenase
Glutathione-dependent formaldehyde-activating enzyme
FAD binding domain
Glutamine amidotransferase class-I
Nitronate monooxygenase
Oxidoreductase NAD-binding domain
Common central domain of tyrosinase
Endoribonuclease L-PSP
Oxidoreductase FAD-binding domain
NUDIX domain
Copper amine oxidase, enzyme domain
Dynamin family
Flavodoxin
Enoyl-(Acyl carrier protein) reductase
Alpha amylase, catalytic domain
Cytochrome P450
Acetyltransferase (GNAT) domain
1.5
1
0.5
0
-0.5
-1
-1.5
Q Category
Q1
Q2
Q3
Q4

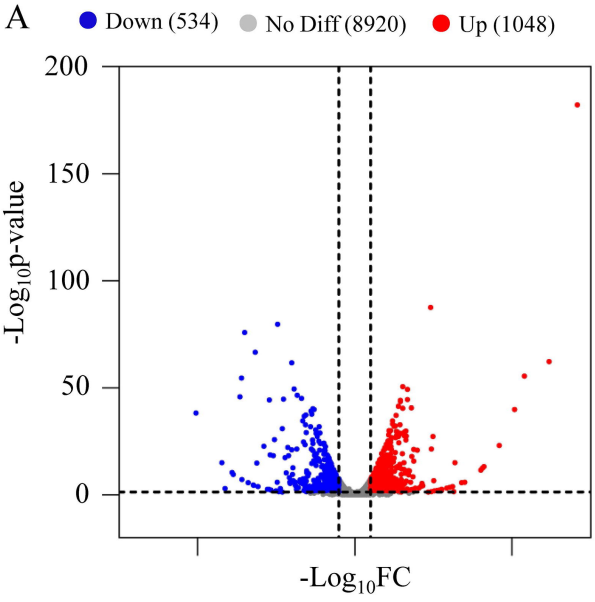
A
Down (534)
No Diff (8920)
Up (1048)
200
150
100
50
0
-Log10p-value
-Log10FC

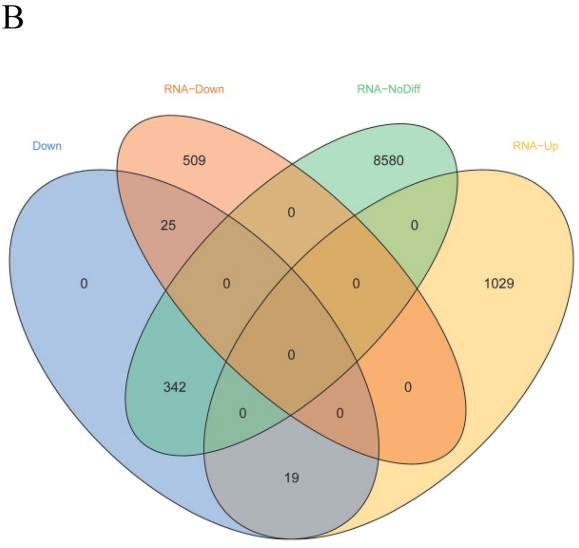
B
Down
RNA-Down
RNA-NoDiff
RNA-Up
0
509
8580
1029
25
0
0
0
0
0
342
0
0
0
19

Table 1 Codon usage of lysine, glutamine and glutamic acid in the Erps.

Amino acid	Biased[a]		Non-Biased[b]		Percentage of Biased (%)	
	Erps	WG	Erps	WG	Erps	WG
Lysine	227	8,337	159	4,489	58.8	65.0
Glutamine	250	6,735	136	6,091	64.8	52.5
Glutamic acid	195	7,443	194	5,383	50.5	58.0

(a: NAA:NAG ratio > 1; b: NAA:NAG ratio ≤ 1.)

Table 2 The *ERPs* functionally studied in *P. oryzae*

Code	Gene ID	Product	Fold Change	Function	Reference
ERP1	MGG_04174	SNF7 family protein	0.76	Vegetative growth, conidiation and pathogenicity, autophagy	(Cheng *et al.* 2018)
ERP2	MGG_10323	GTP-binding protein RHO3	0.73	Appressorial development and pathogenicity	(Zheng *et al.* 2007)
ERP3	MGG_10676	ADP-ribosylation factor 6	0.71	Vegetative growth and conidial morphology	(Zhu *et al.* 2016)
ERP4	MGG_02252	Tetrahydroxynaphthalene reductase MoBuf1	0.64	Conidiation, germination and pathogenicity	(Zhu *et al.* 2021)
ERP5	MGG_04618	Amidophosphoribosyltransferase	0.71	Conidiation and pathogenicity	(Aron *et al.* 2022)
ERP6	MGG_02525	Alanine-glyoxylate aminotransferase	0.49	Appressorial development	(Bhadauria *et al.* 2012a; Bhadauria *et al.* 2012b)